JOURNAL OF CATALYSIS 26, 338-343 (1972)

Structural Study of the Al_2O_3-Promoted Ammonia Synthesis Catalyst

I. Unreduced State

F. GARBASSI, G. FAGHERAZZI, AND M. CALCATERRA

Montecatini Edison Co., "G. Donegani" Research Institute, Novara, Italy

Received November 1, 1971

A structural study of unreduced ammonia synthesis catalyst, singly promoted with alumina, has been performed by means of X-ray diffraction and Mössbauer effect techniques.

The cubic unit cell edge of the spinel lattice of the solid solution of Al_2O_3 in Fe_3O_4 linearly decreases with increasing content of Al. The preference of Al cations for the octahedral B sites of the spinel structure was established at 85% and confirmed by Mössbauer effect.

By means of a study of line broadening, it was possible to reveal the presence of lattice strain, probably resulting from the substitution of Fe^{3+} ions by the smaller Al^{3+} ions.

INTRODUCTION

It is well known that the singly promoted catalyst for the ammonia synthesis process, in the unreduced state, consists of a solid solution of Fe_3O_4 and Al_2O_3, having a spinel-type crystallographic structure (*1*, *2*). Alumina is commonly used in a quantity of about 2% in weight.

In this paper we refer to a structural study, performed with X-ray diffraction and Mössbauer techniques, of singly promoted ammonia catalysts before their reduction to α-Fe. The samples studied had a content of Al between 2 and 10 Al atoms/Fe atoms %.

The structural properties of the unreduced catalyst investigated are:

1. The variation of the length of the edge of the cubic unit cell as a function of Al content.
2. The distribution of Al^{3+} ions between tetrahedral (A) and octahedral (B) sites of the spinel structure.
3. The lattice disorder.

EXPERIMENTAL TECHNIQUES AND METHODS

Samples

The samples of Al-substituted magnetites were prepared by impregnation of a pure magnetite obtained by precipitation with a solution of Al nitrate. Afterwards, the samples were fired at 1000°C for 8 hr in a controlled atmosphere of oxygen (CO/CO_2 mixture) following the method of Economos (*3*). Four samples with 2, 4, 6 and 10% content of Al, in cationic percent, have been studied. All samples were rapidly cooled from a high temperature to room temperature. Before starting with the structural study, the absence of other crystallographic phases, apart from the spinel one, was checked in all samples by X-Ray diffraction, using a Guinier-Nonius camera provided with a monochromator, and recording the spectra under vacuum. For the study of the lattice disorder inside the spinel structure, a reference sample of pure magnetite was annealed at 1000°C in inert atmosphere.

Apparatus

The diffraction patterns for the structural studies concerning the Al^{3+} distribution in the spinel structure were taken with a cylindrical Nonius camera (radius = 57.3 mm) [with the powder sample inside a rotating Lindemann glass capillary of 0.2 mm diameter]. The radiation used was Mn-filtered FeK_α; the intensities were measured from various films, exposed for different times, by means of a Joyce-Loebl CS III microdensitometer using compensation wedges, so that the blackening of the lines was always estimated in the linear part of the density-exposure curve. The average values of the areas of the 14 observed peaks, reported on the same scale, were taken as the observed uncorrected intensities. The angular position of the lines was measured with a linear comparator which could be read to ± 0.02 mm. The Mössbauer spectra were obtained at room temperature using a constant-velocity automatic Elron Electronic Industries spectrometer.* Velocity scans were calibrated by means of the quadrupole splitting of a polycrystalline sample of α-Fe_2O_3. The diffraction spectra for the study of lattice disorder were taken both with a Hilger diffractometer and with a double Guinier-Jagodzinski AEG camera (G-J camera). The diffractometer was provided with proportional counters, discriminator, Soller slits and a receiving slit of 0.1 mm.

The line profiles (400), (200) and (440) were automatically taken on a strip-chart record [velocity: (1/16)°/min] using Mn-filtered FeK_α radiation. The weaker (800) reflection was recorded by automatic point-by-point counting, using Zr-filtered MoK_α radiation with an angular interval between points of 1/16 degrees of 2 ϑ. All diffraction peaks were divided into a large number of intervals; the α_1 peaks were resolved by Rachinger's method (*4*) and the centers of gravity were taken as origins of Fourier analysis. The Fourier coefficients $A(L)$ were obtained with Stokes' method (*5*) studying the profiles as a function of $s = (2 \sin \vartheta)/\lambda$. The films recorded by the G-J camera, provided with a Johannson monochromator, were obtained under vacuum using MoK_{α_1} radiation; Kodirex single emulsion films were employed. Using 0 and $-45°$ orientation for the camera, with respect to the primary beam, it was possible to obtain about 70 different K_{α_1} reflections for the pure magnetite sample. The profiles of the following peaks: (111), (220), (311), (222), (400), (440), (622), (444), (800), (931), (844) and (12.40), were taken into account.

Unit Cell Parameters

The values of the cubic lattice parameter a_0 were obtained by Cohen's least square method (*6*). The asymmetric Straumanis assembly of the film was employed, in order to make the correction for the camera diameter and the film shrinkage.

Al Site Preference

A complete discussion about the methodology employed and its reliability is presented in another paper (*7*).

The precision of measurement of the two characteristic parameters of the spinel structure, namely, the site preference of Al^{3+} ions between A and B sites and the oxygen positional parameter u strongly depends on the experimental accuracy of the observed X-ray line intensities and on the theoretical data concerning the scattering model of the system under consideration. Bearing in mind these two points, we have used the most accurate experimental techniques available in our laboratory and the most recent atomic scattering factors corrected for anomalous dispersion.

For O^{2-} we used the atomic scattering factor derived by Tokonami (*8*), and for Al^{3+}, Fe^{2+} and Fe^{3+}, the values derived by Cromer and Mann (*9*) on the basis of the Hartree–Fock variation model. The observed intensities I_0 were corrected for Lorentz-polarization factors, while the calculated ones I_c were corrected for multiplicity and the Debye–Waller factor. On the assumption that the substituted trivalent cation statistically replaces Fe^{3+}, the

* Measurements taken at Weizmann Institute, Rehovot, Israel.

calculated intensities are functions only of the oxygen positional parameter u and of the cationic distribution parameter x, defined by us as the percentage of the Al^{3+} ions occupying the B sites of the spinel structure (space group $Fd3m$). The observed reflections of the powder spectra were: (111), (220), (311), (222), (400), (422), (333)–(511), (440), (533), (622), (444), (642), (553)–(731), (800).

The values of u and x obtained by minimizing the residual

$$R' = \sum_{hkl} [(i_0^{hkl})^{1/2} - (i_c^{hkl})^{1/2}]^2,$$

were taken as the solutions of the two parameters under study. In this expression i_0 is the corrected observed intensity and i_c is equal to $\Sigma m_{hkl} F_c^2(hkl)$, with m_{hkl} the multiplicity factor for each (hkl) line, $F_c(hkl)$ the calculated structure factors (*10*) and with the sum extended to all (hkl) reflections having the same values of $(h^2 + k^2 + l^2)$. The minimum of R' was found by numerical methods using a nonlinear automatic optimum seeking procedure (*11*), starting from the minimum of the conventional R residual defined as:

$$R = \frac{\Sigma_{hkl}[(i_0^{hkl})^{1/2} - (i_c^{hkl})^{1/2}]}{\Sigma_{hkl}(i_c^{hkl})^{1/2}}.$$

All calculations were performed by a UNIVAC 1108 computer.*

Lattice Disorder

The determination of the root square (rms) strain $\langle \epsilon^{22} \rangle^{1/2}$ and the effective crystallite size D_{eff} was performed by two methods:

1. By starting from the two pairs of lines (220)–(440) and (400)–(800) obtained by the diffractometer, determining the Fourier cosine coefficients $A(L)$ with the Stokes method and then applying the Warren-Averbach method (*12*).

2. By plotting the corrected integral breadth, defined as the ratio between peak area and maximum intensity of the K_{α_1} peaks obtained by the G-J camera. The experimental integral breadths were corrected for the instrumental broadening, using a Cauchy square function: $[1 + K s^2]^{-2}$, where K is a constant and $s = (2 \sin \vartheta/\lambda)$ the reciprocal space variable, as the analytical curve describing the profiles of both the experimental broadened peak and the reference peak. The reference peak was obtained from a pure magnetite sample annealed at 1000°C, which was broadened only for instrumental reasons (*13*).

Starting from the true β values of the corrected peaks, the broadening due to the effective crystallite sizes D_{eff} was separated from the broadening due to the strain $\langle \epsilon \rangle$, using the relation (*14*):

$$\left(\frac{\beta(s)}{\lambda}\right)^2 = \frac{1}{D_{\text{eff}}^2} + 4\langle \epsilon \rangle^2 s^2$$

where $2\vartheta_0$ is the angular position of the K_{α_1} peak barycenter, and λ is the wavelength of the radiation used.

Results and Discussion

Figure 1 and Table 1 show the variation of the lattice constant a_0 as a function of the content t of Al in the solid solution $Fe_{3-t}\ Al_tO_4$. The curve follows Vegard's

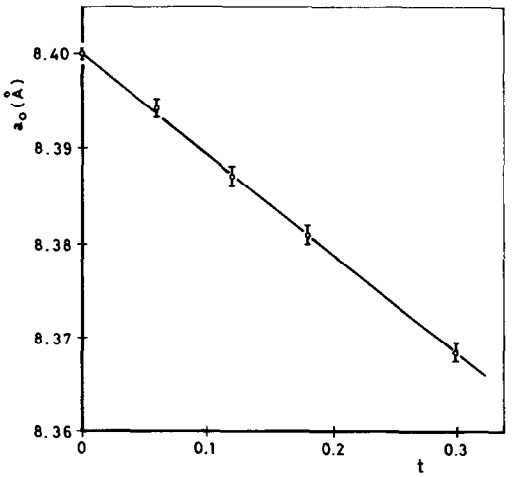

FIG. 1. Lattice parameter a_0 versus amount of substitutional Al^{3+}.

* Programs used were the following: A. Angelini—STOKES (Fourier analysis of diffraction profiles); G. Buzzi-Ferraris—OPTVIN (numerical minimization of R'); F. Garbassi—PROTEO (lattice parameters); REFLEX (barycenter of the peaks and Rachinger separation); DISCAT (cation distribution).

TABLE 1
LATTICE PARAMETERS OF PURE AND Al-SUBSTITUTED MAGNETITES

Sample	Lattice parameter a_0(Å)
Pure magnetite	8.3999 ± 0.0005
2% Al-substituted magnetite	8.394 ± 0.001
4% Al-substituted magnetite	8.387 ± 0.001
6% Al-substituted magnetite	8.381 ± 0.001
10% Al-substituted magnetite	8.369 ± 0.001

linear law in agreement with other authors (*15*, *16*) and the shrinkage can be easily explained bearing in mind that the ionic radius of Al^{3+} is smaller than that of Fe^{3+} [e.g., $r_{Al}^{3+} = 0.51$ Å, $r_{Fe}^{3+} = 0.64$ Å, according to Ahrens (*17*)]. The length of the cell edge for the pure synthetic magnetite is slightly different from that found by other authors (*18–20*) and this could depend on the preparation method (*21*). Figure 2 gives the diagram of the conventional residual factor R as a function of u and x for the 10% Al substituted magnetite ($t = 0.3$). The minimum of the residual factor R' was found for $u = 0.384 \pm 0.0015$ and $x = 85 \pm 5$. For the reference sample of pure magnetite we have obtained, for the oxygen parameter, a value of $u = 0.382 \pm 0.001$.

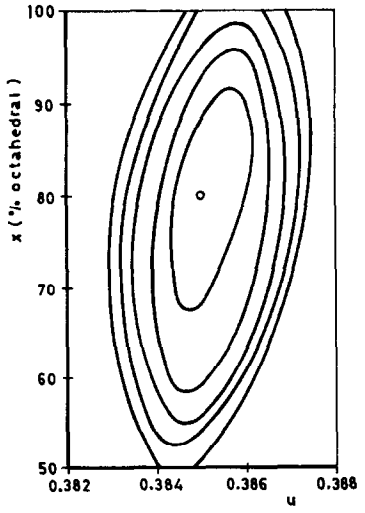

FIG. 2. R' (u, x) diagram for the 10% Al-substituted magnetite. Contour lines indicate 0.1 increments in R' value starting from minimum point.

Mössbauer spectra of pure, 2% Al- and 10% Al-substituted magnetites show a broadening of the B peak pertaining to octahedral sites as the Al substitution is increased. This broadening is due to a distribution of several values of the hyperfine internal magnetic field around its average value, caused by the existence of different situations in the tetrahedral sites. This fact could occur in our sample assuming that a small fraction of the Al^{3+} ions is present in these sites. In fact, each A site is surrounded by twelve B sites, while each B site is surrounded by only six A sites. Therefore, it is evident that the substitution of an Fe^{3+} ion by an Al^{3+} ion in a tetrahedral site produces a much greater decrease of the superexchange interaction, than a substitution in an octahedral site. This variation causes a broadening of the B peak, the effective magnetic field being proportional to ionic moments (*7*, *22*).

Thus the Mössbauer results are consistent with the X-ray determination of the cation distribution. Figure 3 reports spectra and hyperfine internal magnetic fields values for pure and substituted magnetite samples. The formula of a 10% Al-substituted magnetite can therefore be written as:

$$Fe^{3+}_{0.955}Al^{3+}_{0.045}[Fe^{2+}Fe^{3+}_{1.745}Al^{3+}_{0.255}]\ O_4^{2-},$$

where ions in B sites are indicated between brackets. It is well known that the ideal oxygen positional parameter u of an undistorted spinel structure corresponds to:

$$u_{id} = 0.375.$$

In our case, $u > u_{id}$, and this displacement of the oxygen ion makes the tetrahedral sites larger and the octahedral sites smaller. The radii of the spheres in A and B sites are respectively (*23*):

$$r_A = \left(u - \frac{1}{4}\right) a_0\sqrt{3} - R_0,$$

$$r_B = \left(\frac{5}{8} - u\right) a_0 - R_0,$$

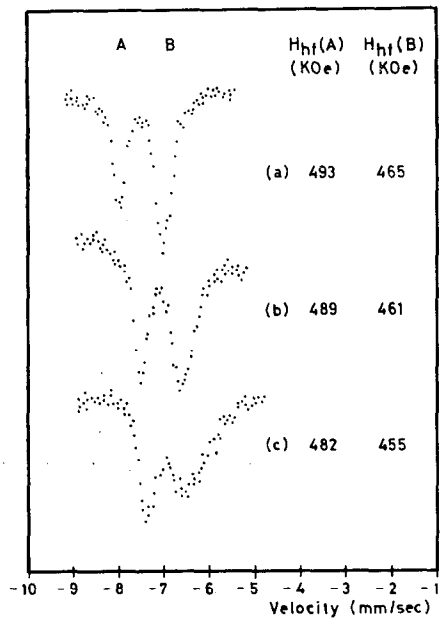

FIG. 3. First lines of the Mössbauer spectra, attributed to tetrahedral (A) and octahedral (B) sites in the spinel structure. Values of internal hyperfine magnetic fields H_{hf} and spectra for pure (a), 2% Al-substituted (b) and 10% Al-substituted magnetite (c) are reported.

where R_0 is the oxygen ion radius. Assuming a value of 1.32 Å for R_0 (*24*), we obtain for our sample $r_A = 0.622$ Å and $r_B = 0.697$ Å instead of $r_A = 0.600$ Å and $r_B = 0.721$ Å pertinent to the pure magnetite. The shrinkage of the octahedral sites is probably due to the stronger preference for B sites found for the smaller Al^{3+} ions compared with larger Fe^{3+} ions.

The insertion of Al cations in the spinel lattice gives rise to local distortions which were detected by X-ray diffraction line broadening. In Fig. 4, we report the plots of Fourier cosine coefficients $A(L)$ as a function of L, for the two pairs of reflections (220)–(440) and (400)–(800) of the sample containing 10% Al. From these plots we have calculated, following the method of Warren–Averbach (*12*), the values of rms strain $\langle \epsilon_L^2 \rangle^{1/2}$ (Fig. 5) and the values of the effective crystallite sizes D_{eff} in the crystallographic directions [100] and [110] (Table 2). In Fig. 6, we report the plot of integral breadths for the same sample, from which an isotropic distribution of the strain in all crystallographic directions can be deduced. It is worth noticing that the values for the strain obtained by the two different methods are very close to each other. On the other hand, a discrepancy was found in the average particle size. As known, the values obtained with the Warren–Averbach method are the most reliable.

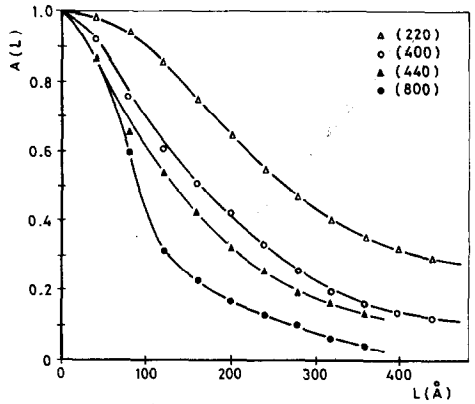

FIG. 4. Fourier cosine coefficients $A(L)$, corrected after Stokes, as functions of L(Å).

In Table 2, we report the values of the strain obtained also for 2% Al-substituted magnetite. The decrease of the value for the strain confirms, for our range of substitution, the direct dependence of structural disorder on the content of substitutional Al.

ACKNOWLEDGMENTS

Thanks are due to Mr. F. Lazzerin for the preparation of the samples.

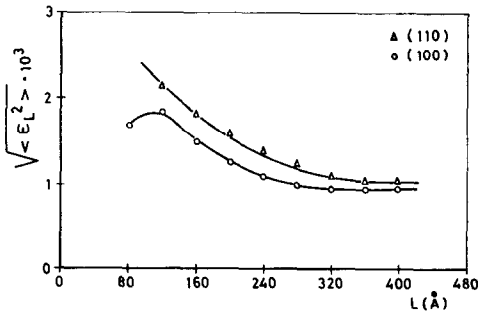

FIG. 5. Average strain $\langle \epsilon^2 \rangle^{1/2}$ as a function of L(Å) along the crystallographic directions [100] and [110].

TABLE 2
STRAIN AND PARTICLE SIZE OF Al-SUBSTITUTED MAGNETITES

Method:	Warren–Averbach		Integral breadths (averaged)	
Crystallographic direction:	[100]	[110]		
Amount of substituent (%):	10	10	10	2
rms strain $\langle \epsilon^2 \rangle^{1/2}$	1×10^{-3}	1.1×10^{-3}	1.2×10^{-3}	0.3×10^{-3}
Av particle size D_{eff}	420	530	840	nd

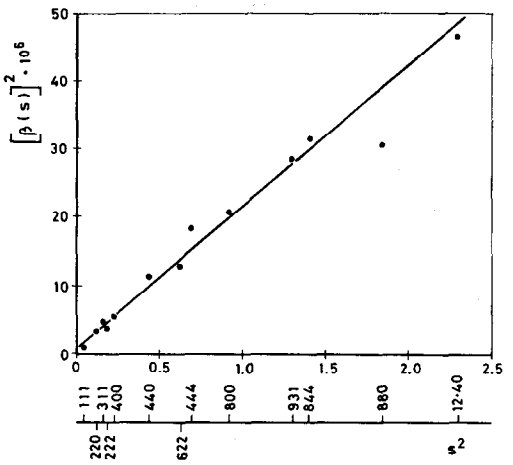

FIG. 6. Integral breadth as function of reciprocal space variable.

REFERENCES

1. WYCKOFF, R. W. G., AND CRITTENDEN, E. D., *J. Amer. Chem. Soc.* **47**, 2866 (1925).
2. BRILL, R., *Z. Elektrochem.* **38**, 669 (1932).
3. ECONOMOS, G., *J. Amer. Ceram. Soc.* **38**, 241 (1955).
4. RACHINGER, W. A., *J. Sci. Instrum.* **25**, 254 (1948).
5. STOKES, A. R., *Proc. Phys. Soc., London* **61**, 382 (1948).
6. COHEN, M. U., *Rev. Sci. Instrum.* **6**, 68 (1935); **7**, 155 (1936).
7. FAGHERAZZI, G., AND GARBASSI, F., *J. Appl. Crystallogr.* **5**, 18 (1972).
8. TOKONAMI, M., *Acta Crystallogr.* **19**, 486 (1965).
9. CROMER, D. T., AND MANN, J. B., *Acta Crystallogr. Sect. A* **24**, 312 (1968).
10. BUERGER, M. J., *in* "Crystal-structure analysis," p. 261. Wiley, New York, 1960.
11. BUZZI FERRARIS, G., *Quad. Ing. Chim. Ital.* **4**, 171 and 180 (1968).
12. WARREN, B. E., AND AVERBACH, B. L., *J. Appl. Phys.* **21**, 595 (1950) and **23**, 497 (1952).
13. FAGHERAZZI, G., AND LANZAVECCHIA, G., *Mater. Sci. Eng.* **5**, 63 (1969/70).
14. WAGNER, C. N. J., AND AQUA, E. N., *in* "Advances in X-ray Analysis," Vol. **7**, p. 46, Plenum, New York, 1964.
15. WESTRIK, R., *J. Chem. Phys.* **21**, 2094 (1953).
16. DRY, M. E., AND FERREIRA, L. C., *J. Catal.* **7**, 352 (1967).
17. AHRENS, L. M., *Geochim. Cosmochim. Acta* **2**, 155 (1952).
18. BASTA, E. Z., *Mineral. Mag.* **31**, 431 (1957).
19. ROOKSBY, H. P., *in* "The X-Ray Identification and Crystal Structure of Clay Minerals." Mineralogical Society, London, 1961.
20. O'REILLY, W., *Acta Crystallogr. Sect. B* **24**, 422 (1968).
21. COLOMBO, U., FAGHERAZZI, G., GAZZARRINI, F., LANZAVECCHIA, G., AND SIRONI, G., *Ind. Chim. Belge* **32**, 337 (1967).
22. SAWATSKY, G. A., VAN DER WOUDE, F., AND MORRISH, A. M., *J. Appl. Phys.* **39**, 1204 (1968).
23. SMIT, J., AND WIJN, H. P. J., *in* "Ferrites," p. 140. Philips Technical Library, Eindhoven, The Netherlands, 1965.
24. "Handbook of Chemistry and Physics." Chem. Rubber Co., Cleveland, OH. (1969/70).